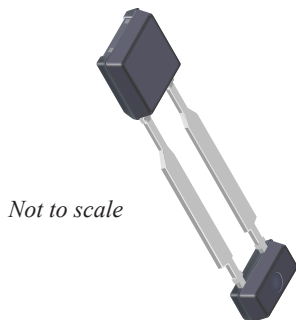


Two-Wire, Differential, Vibration-Resistant Sensor IC with Speed and Direction Output

FEATURES AND BENEFITS

- Integrated IC and capacitor, single overmolded package to reduce external EMI-protection requirements
- Two-wire, pulse-width output protocol
- Highly configurable output protocol options
- Digital output representing target profile
- Speed and direction information of target
- Vibration tolerance
 - Small-signal lockout for small amplitude vibration
 - Proprietary vibration detection algorithms for large amplitude vibration
- Air-gap-independent switchpoints
- Large operating air gap capability
- Undervoltage lockout
- True zero-speed operation
- Wide operating voltage range
- AEC-Q100 automotive qualified
- Robust test-coverage capability with Scan Path and IDDQ measurement

Package: 2-Pin SIP (Suffix UB)



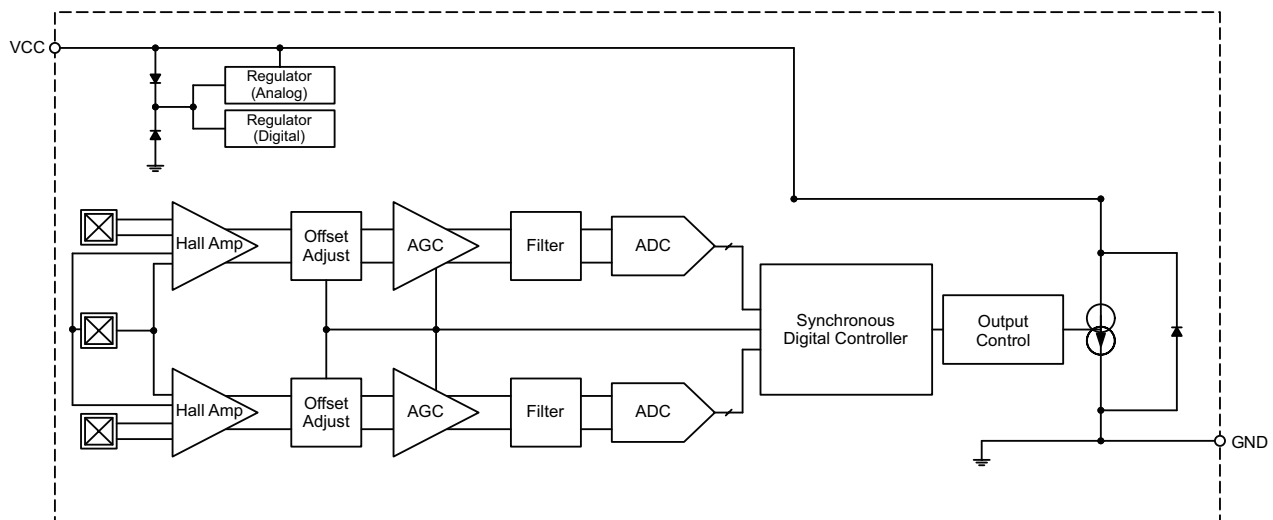
DESCRIPTION

The A1699 is an optimized Hall-effect integrated circuit (IC) that provides a user-friendly solution for direction detection and true zero-speed, digital ring-magnet sensing. The small package can be easily assembled and used in conjunction with a wide variety of target sensing applications.

The IC employs patented algorithms for the special operational requirements of automotive transmission applications. The speed and direction of the target are communicated through a variable pulse-width output protocol. The A1699 is particularly adept at handling vibration without sacrificing maximum air gap capability or creating any erroneous direction information. The advanced vibration detection algorithm will systematically calibrate the sensor IC on the initial magnetic poles of true target rotation and not on vibration, always guaranteeing an accurate signal in running mode.

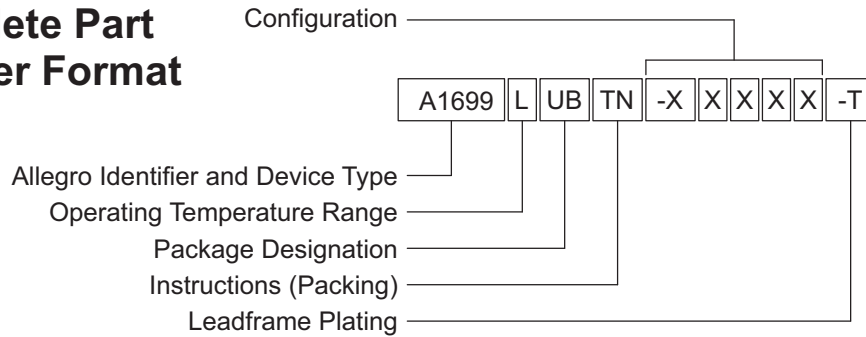
Advanced signal processing and innovative algorithms make the A1699 an ideal solution for a wide range of speed- and direction-sensing needs.

The A1699 is provided in a 2-pin miniature SIP package (suffix UB) that is lead (Pb) free, with tin leadframe plating. The UB package includes an IC and capacitor integrated into a single overmolded package to reduce external EMI protection requirements.



Functional Block Diagram

Complete Part Number Format



Allegro Identifier and Device Type		[A1699]
Operating Temperature Range		[L]
Package Designation		[UB] 2-pin plastic SIP
Instructions (Packing)		[TN] Tape and reel
Configuration	Rotation Direction	[-F] pin 1-to-2 forward or [-R] pin 2-to-1 forward
	Number of Pulses	[S] single, one pulse per magnetic pole pair or [D] dual, one pulse for each north and south pole
	Reverse Pulse Width	[N] 90 μs (narrow) or [W] 180 μs (wide)
	Calibration Pulses	[B] Blanked, no output during Calibration or [P] Pulses during Calibration
	Vibration Immunity / Direction Change	[L] Low vibration immunity with immediate direction change detection or [H] High vibration immunity with non-direction pulses
Leadframe Plating		[T] Lead (Pb) free

For example: A1699LUBTN-RSNPL-T

Where a configuration character is unspecified, “x” will be used. For example, -xSNPL applies to both Rotation Direction configuration variants.

A1699

Two-Wire, Differential, Vibration-Resistant Sensor IC with Speed and Direction Output

SELECTION GUIDE

Part Number	Packing*
A1699LUBTN-xxxxx-T	4000 pieces per 13-in. reel



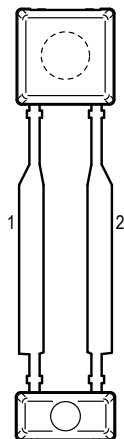
*Contact Allegro™ for additional packing options.

ABSOLUTE MAXIMUM RATINGS*

Characteristic	Symbol	Notes	Rating	Unit
Supply Voltage	V_{CC}	Refer to Power Derating Section	28	V
Reverse Supply Voltage	V_{RCC}		-18	V
Operating Ambient Temperature	T_A	L temperature range	-40 to 150	°C
Maximum Junction Temperature	$T_{J(max)}$		165	°C
Storage Temperature	T_{stg}		-65 to 170	°C

INTERNAL DISCRETE CAPACITOR RATINGS

Characteristic	Symbol	Test Conditions	Value (Typ.)	Unit
Nominal Capacitance	C_{SUPPLY}	Connected between VCC and GND	10000	pF



Terminal List Table

Name	Number	Function
VCC	1	Supply Voltage
GND	2	Ground

Package UB, 2-Pin SIP Pinout Diagram

OPERATING CHARACTERISTICS: Valid throughout full operating and temperature ranges, unless otherwise specified

Characteristic	Symbol	Test Conditions	Min.	Typ. ¹	Max.	Unit
ELECTRICAL CHARACTERISTICS						
Supply Voltage ²	V_{CC}	Operating, $T_J < T_{J(max)}$	4	–	24	V
Undervoltage Lockout	$V_{CC(UV)}$	V_{CC} transitioning from 0 → 5 V or 5 → 0 V	–	3.6	3.95	V
Reverse Supply Current ³	I_{RCC}	$V_{CC} = V_{RCC(max)}$	–	–	–10	mA ³
Supply Zener Clamp Voltage	$V_{ZSUPPLY}$	$I_{CC} = I_{CC(max)} + 3 \text{ mA}$, $T_A = 25^\circ\text{C}$	28	–	–	V
Supply Current	$I_{CC(Low)}$	Low-current state (running mode)	5	–	8	mA
	$I_{CC(High)}$	High-current state (running mode)	12	–	16	mA
	$I_{CC(SU)}$ (LOW)	Low-current level (calibration) and Power-on mode	5	–	8.5	mA
Supply Current Ratio	$I_{CC(High)}/I_{CC(Low)}$	Measured as a ratio of high current to low current	1.9	–	–	–
OUTPUT						
Output Rise Time	t_r	$\Delta I/\Delta t$ from 10% to 90% I_{CC} level; Corresponds to measured output slew rate with C_{SUPPLY}	–	2	4	μs
Output Fall Time	t_f	$\Delta I/\Delta t$ from 90% to 10% I_{CC} ; Corresponds to measured output slew rate with C_{SUPPLY}	–	2	4	μs
OUTPUT PULSE CHARACTERISTICS⁴						
Pulse Width, Forward Rotation	$t_{w(FWD)}$		38	45	52	μs
Pulse Width, Reverse Rotation	$t_{w(REV)}$	-xxNxx variant	76	90	104	μs
		-xxWxx variant	153	180	207	μs
Pulse Width, Non-Direction	$t_{w(ND)}$	-xxNPx and -xxNxH variants	153	180	207	μs
		-xxWPx and -xxWxH variants	306	360	414	μs

Continued on the next page...

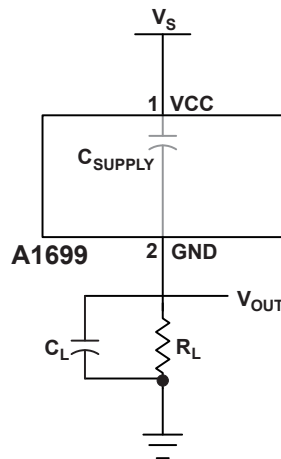


Figure 1: Typical Application Circuit

OPERATING CHARACTERISTICS (continued): Valid throughout full operating and temperature ranges, unless otherwise specified

Characteristic	Symbol	Test Conditions	Min.	Typ. ¹	Max.	Unit	
INPUT MAGNETIC CHARACTERISTICS							
Allowable Differential Sequential Signal Variation	$B_{SEQ(n+1)} / B_{SEQ(n)}$	Signal cycle-to-cycle variation (see Figure 3)	0.6	–	–	–	
	$B_{SEQ(n+i)} / B_{SEQ(n)}$	Overall signal variation (see Figure 3)	0.4	–	–	–	
CALIBRATION							
First Direction Output Pulse ⁶		Amount of target rotation (constant direction) following power-on until first electrical output pulse of either $tw_{(FWD)}$ or $tw_{(REV)}$. See Figure 2	$B_{IN} > 60 G_{PP}$ $B_{IN} \leq 1200 G_{PP}$	–	$2 \times T_{TARGET}$	$<3 \times T_{TARGET}$	degrees
			$30 G_{PP} \leq B_{IN}$ $B_{IN} \leq 60 G_{PP}$	–	$2.5 \times T_{TARGET}$	$<4 \times T_{TARGET}$	degrees
First Direction Pulse Output Following Direction Change	N_{CD}	Amount of target rotation (constant direction) following event until first electrical output pulse of either $tw_{(FWD)}$ or $tw_{(REV)}$. $V_{SP(sep)} \geq 35$. See Figure 2	-xxxxL variant	–	1	–	switch-point
			-xxxxH variant	$1 \times T_{TARGET}$	$2 \times T_{TARGET}$	$3 \times T_{TARGET}$	degrees
First Direction Pulse Output Following Running Mode Vibration		Amount of target rotation (constant direction) following event until first electrical output pulse of either $tw_{(FWD)}$ or $tw_{(REV)}$. See Figure 2	-xxxxL variant	–	–	$1.25 \times T_{TARGET}$	degrees
			-xxxxH variant	$1 \times T_{TARGET}$	$2 \times T_{TARGET}$	$3 \times T_{TARGET}$	degrees
Switch Point Separation	$V_{SP(sep)}$	Minimum separation between channels as a percentage of signal amplitude at each switching point. See Figure 2	20	–	–	% pk-pk	

⁶ Power-up frequencies ≤ 200 Hz. Higher power-on frequencies may require more input magnetic cycles until output edges are achieved.

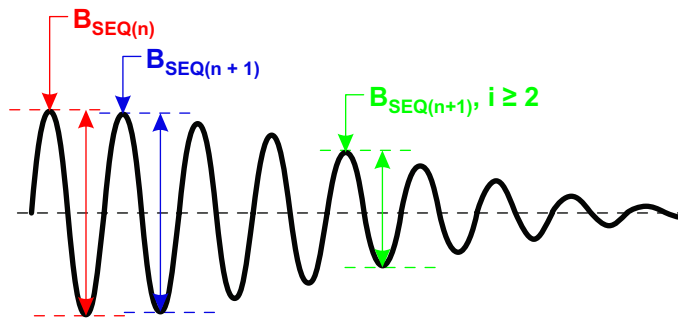


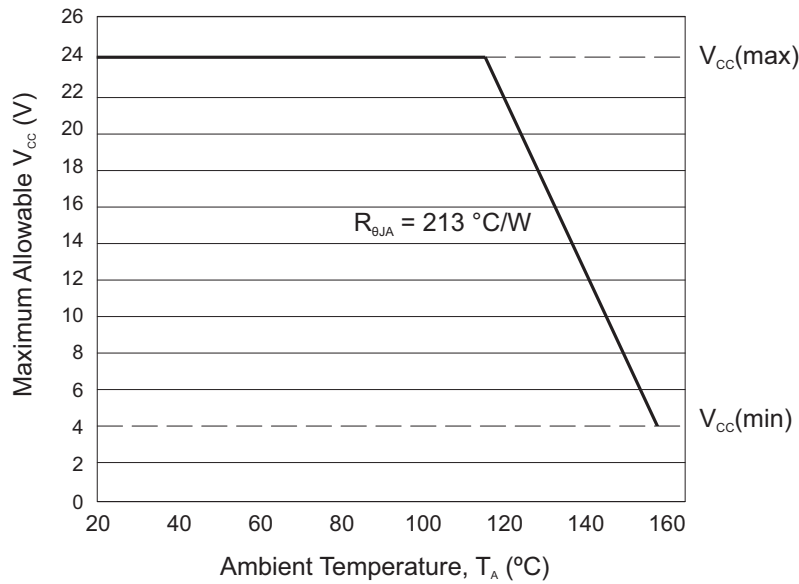
Figure 3: Differential Signal Variation

THERMAL CHARACTERISTICS

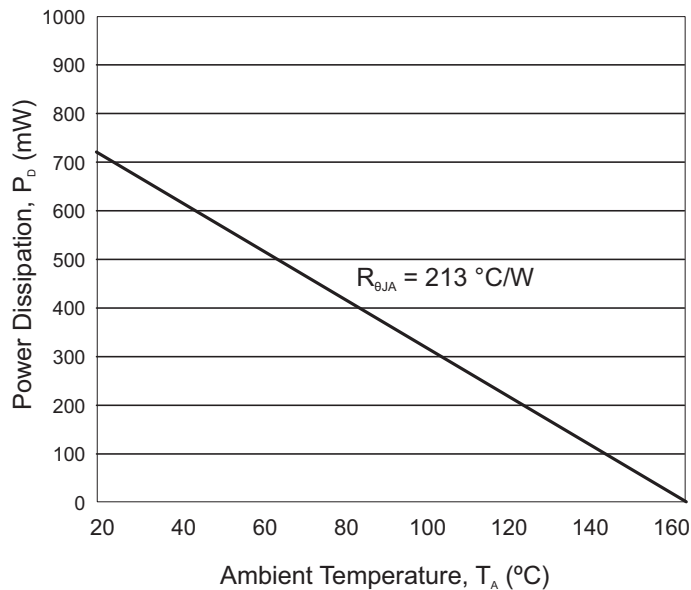
Characteristic	Symbol	Test Conditions*	Value	Unit
Package Thermal Resistance	$R_{\theta JA}$	Single-layer PCB with copper limited to solder pads	213	$^{\circ}\text{C}/\text{W}$

*Additional thermal information is available on the Allegro website.

Power Derating Curve

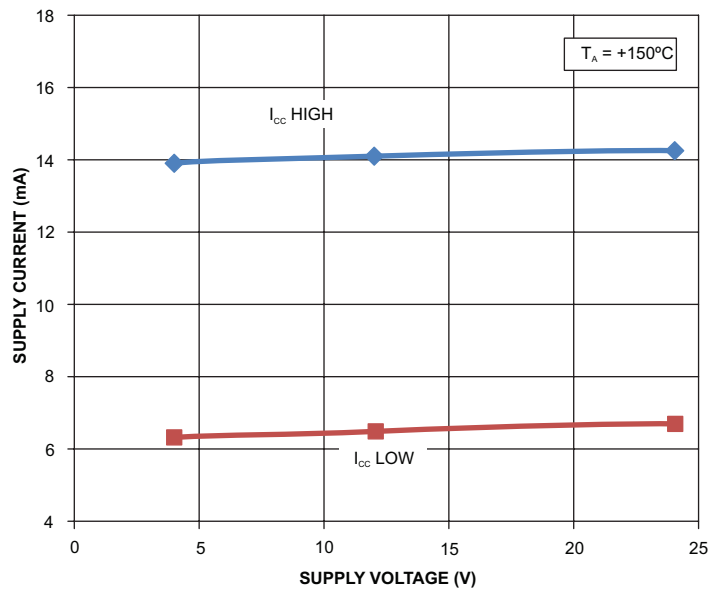
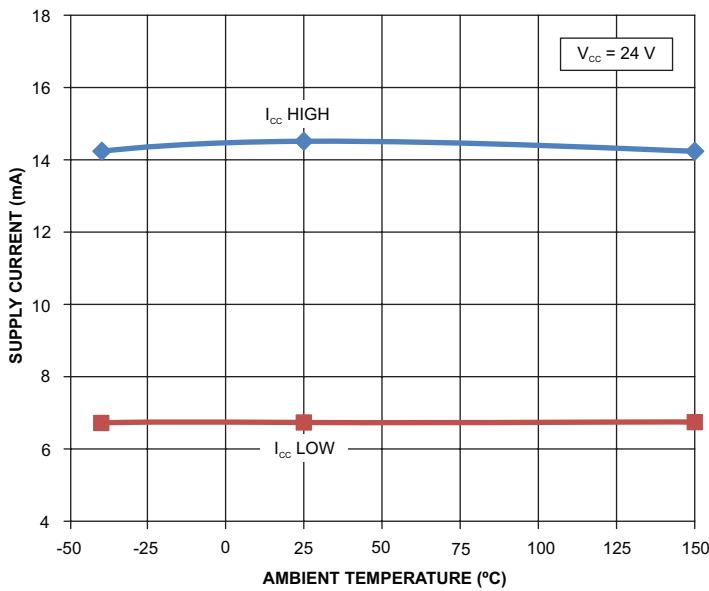
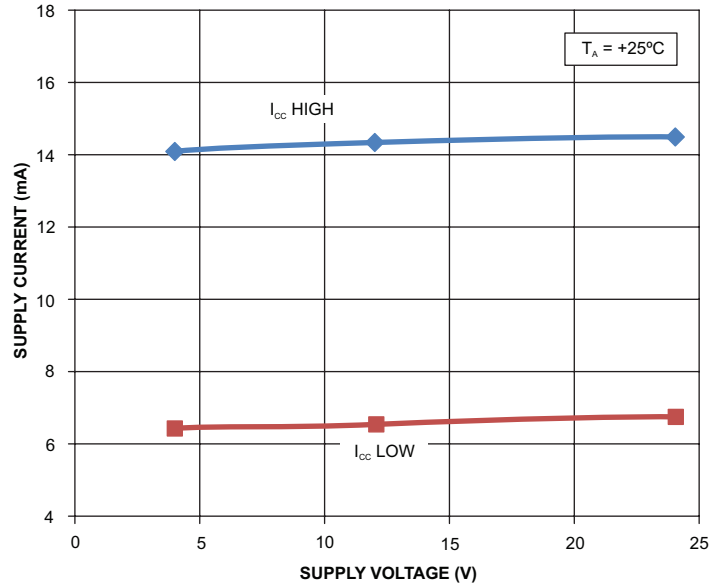
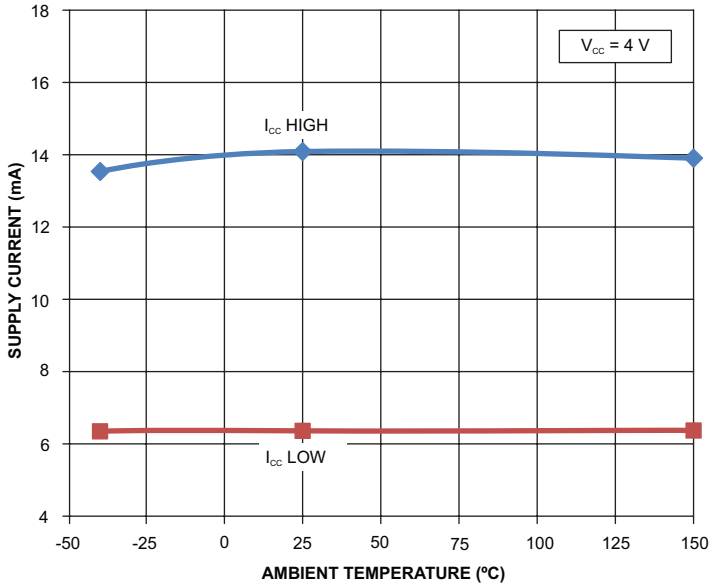


Power Dissipation versus Ambient Temperature

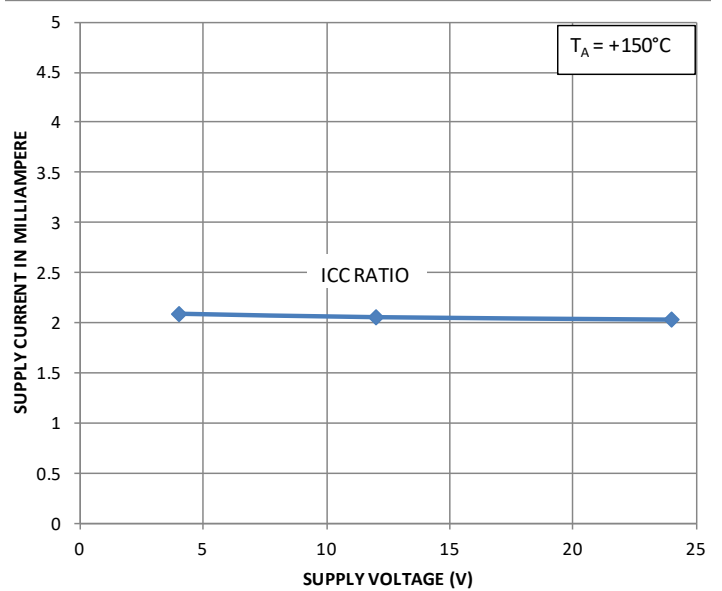
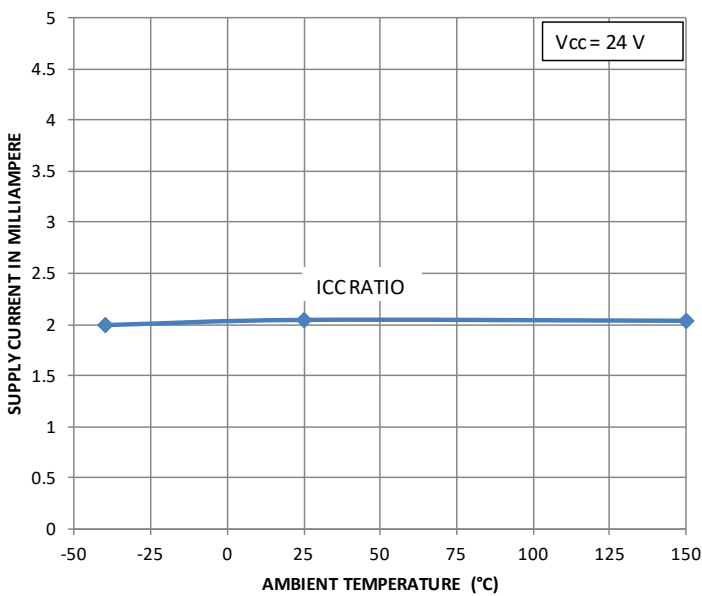
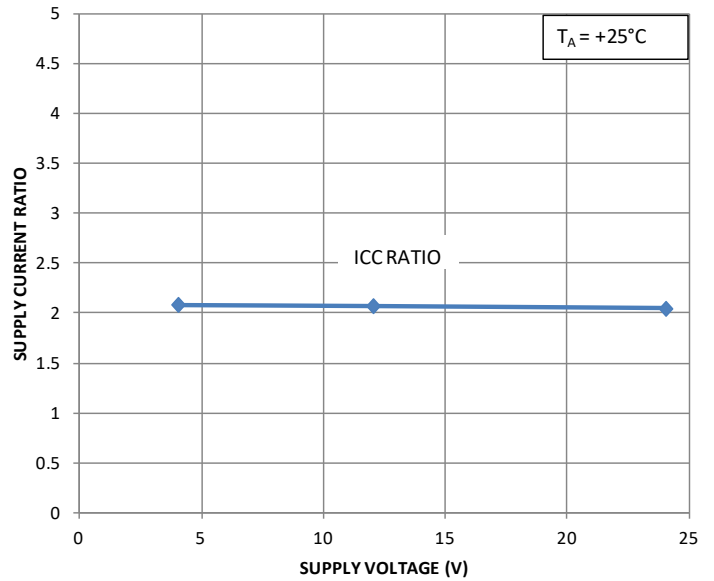
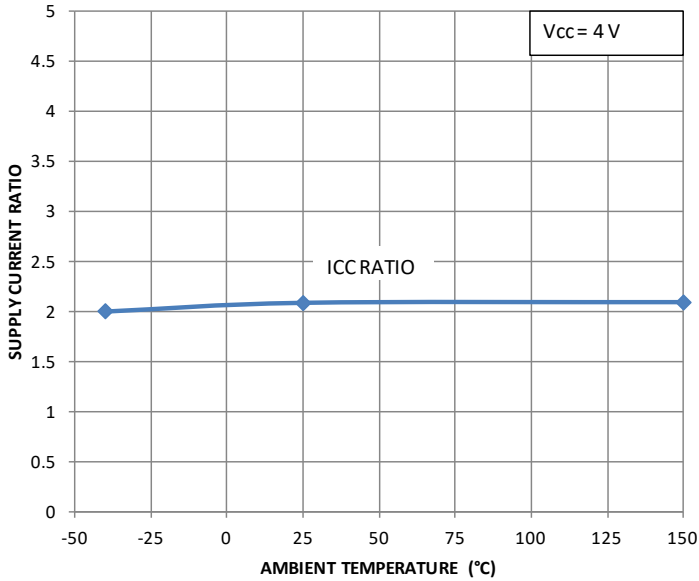


CHARACTERISTIC PERFORMANCE

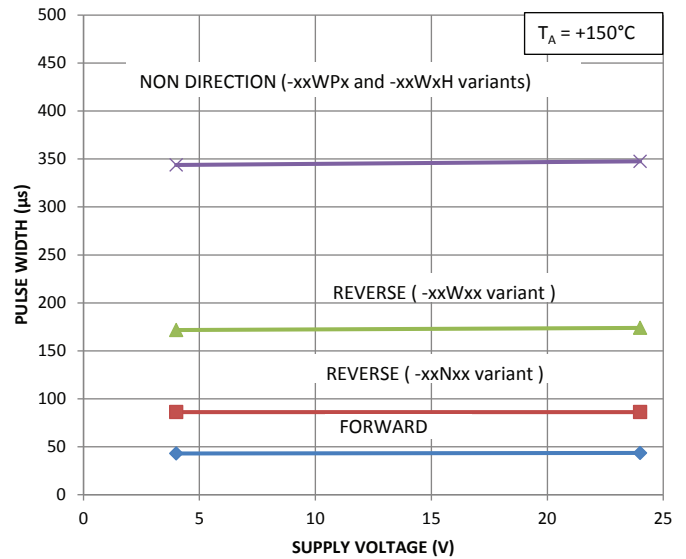
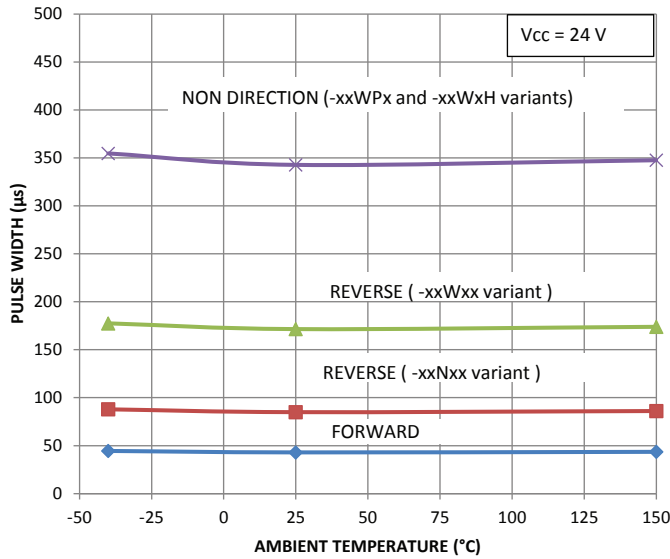
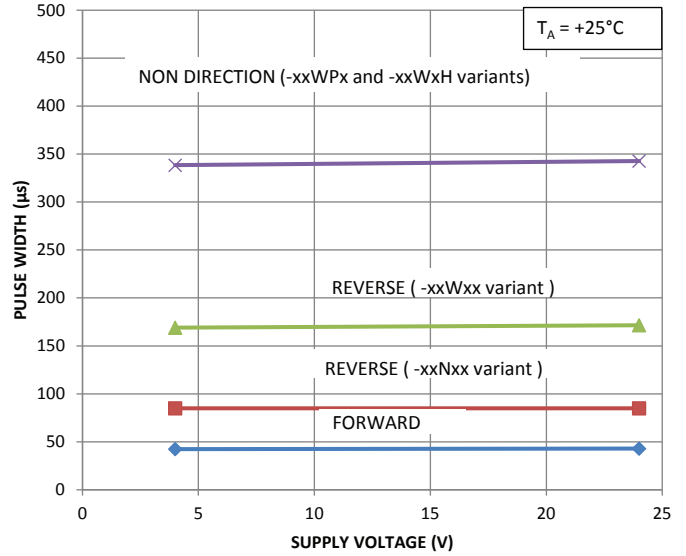
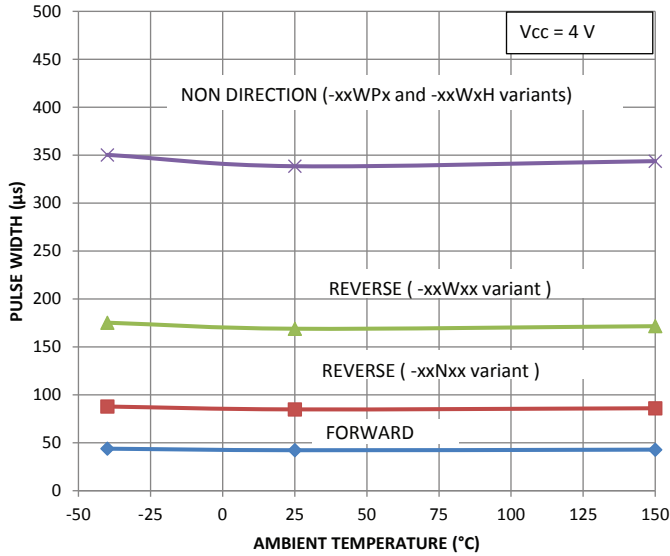
Supply Current



Supply Current Ratio



Pulse Width



FUNCTIONAL DESCRIPTION

Sensing Technology

The sensor IC contains a single-chip Hall-effect circuit that supports a trio of Hall elements. These elements are used in differential pairs to provide electrical signals containing information regarding edge position and direction of target rotation. The A1699 is intended for use with ring magnet and gear targets.

After proper power is applied to the sensor IC, it is capable of providing digital information that is representative of the magnetic features of a rotating target. The waveform diagrams in Figure 4 present the automatic translation of the target profiles to the digital output signal of the sensor IC

Direction Detection

The sensor IC compares the relative phase of its two differential channels to determine which direction the target is moving. The relative switching order is used to determine the direction, which is communicated through the output protocol.

Data Protocol Description

When a target passes in front of the device (opposite the branded face of the package case), the A1699 generates an output pulse(s) for each pair of magnetic poles of the target. Speed information is provided by the output pulse rate, while direction of target rotation is provided by the duration of the output pulses. The sensor IC can sense target movement in both the forward and reverse directions.

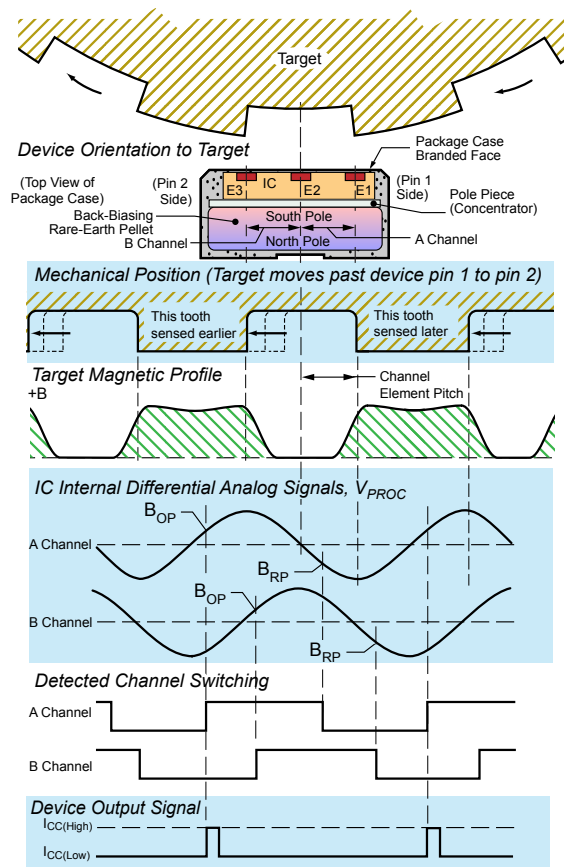
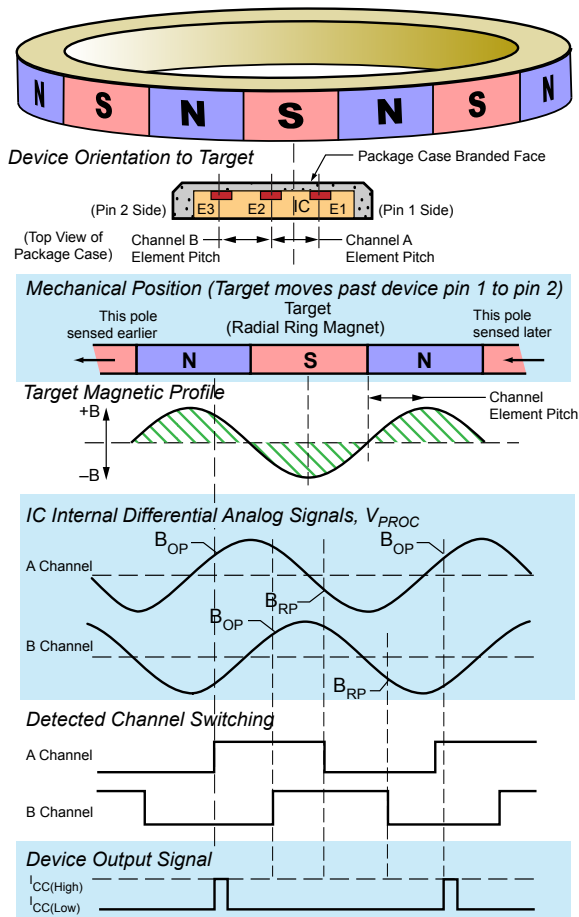


Figure 4: The magnetic profile reflects the features of the target, allowing the sensor IC to present an accurate digital output (-xSxxx variant shown).

Forward Rotation (see Figure 5)

When the target is rotating such that a magnetic pole near the sensor IC (of -Fxxxx variant) passes from pin 1 to pin 2, this is referred to as forward rotation. This direction is opposite for the -Rxxxx variant. Forward rotation is indicated by output pulse widths of $t_{w(FWD)}$ (45 μ s typical).

Reverse Rotation (see Figure 5)

When the target is rotating such that a magnetic pole passes from pin 2 to pin 1, it is referred to as reverse rotation for the -Fxxxx variant. This direction is opposite for the -Rxxxx variant. Reverse rotation is indicated by output pulse widths of $t_{w(REV)}$ (90 μ s typical for -xxNxx variant, or 180 μ s typical for -xxWxx variant).

Timing

As shown in Figure 6, the pulse appears at the output slightly before the sensed magnetic edge traverses the package branded

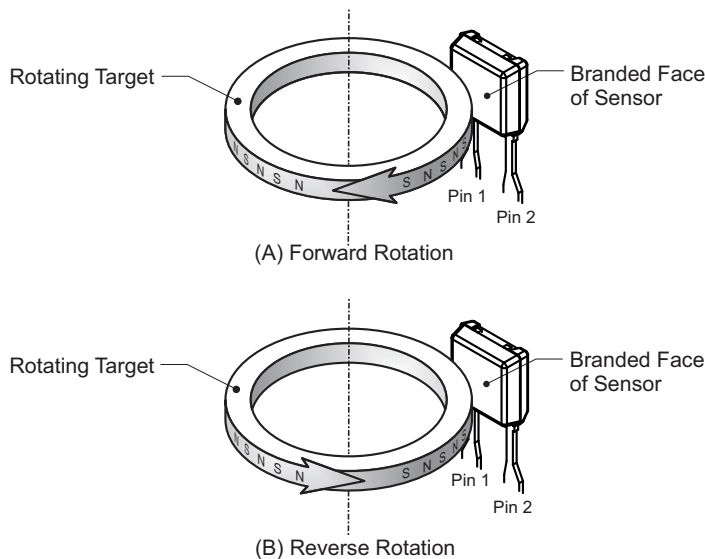


Figure 5: Target Rotation for -Fxxxx Variant.
-Rxxxx variant inverts detected direction of rotation.

face. For targets rotating from pin 2 to 1, this shift (Δ_{fwd} with R variants, with south pole of backbiasing pellet toward IC) results in the pulse corresponding to the valley with the sensed mechanical edge; for targets rotating from pin 1 to 2, the shift (Δ_{rev}) results in the pulse corresponding to the tooth with the sensed edge. Figure 7 shows pulse timing for F variants. The sensed mechanical edge that stimulates output pulses is kept the same for both forward and reverse rotation by using only one channel to control output switching.

Direction Validation

For the -xxxxL variant, following a direction change in running mode, direction changes are immediately transmitted to the output.

For the -xxxxH variant, following a direction change in running mode, output pulses have a width of $t_{w(ND)}$ until direction information is validated.

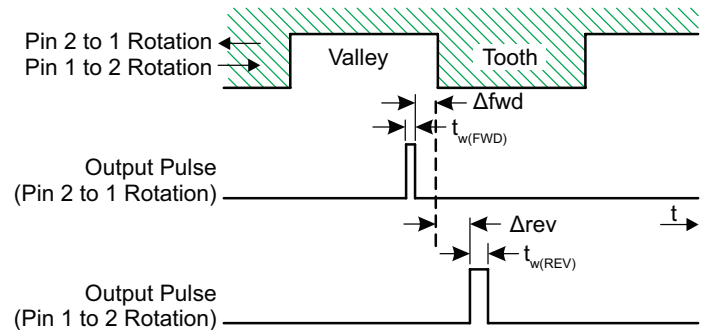


Figure 6: Output Protocol (-RSxxxx variant)

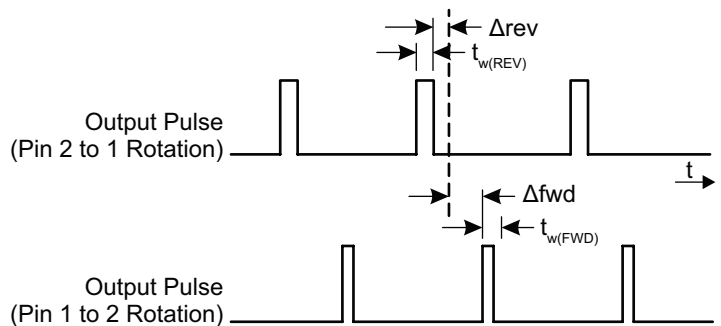


Figure 7: Output Protocol (-FDxxxx variant)

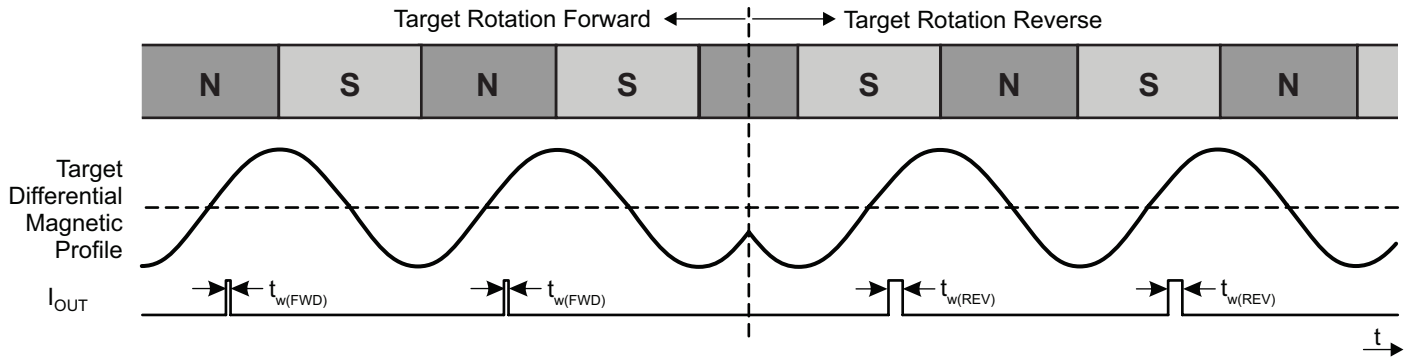


Figure 8: Example Running Mode Direction Change (-FSxxL variant)

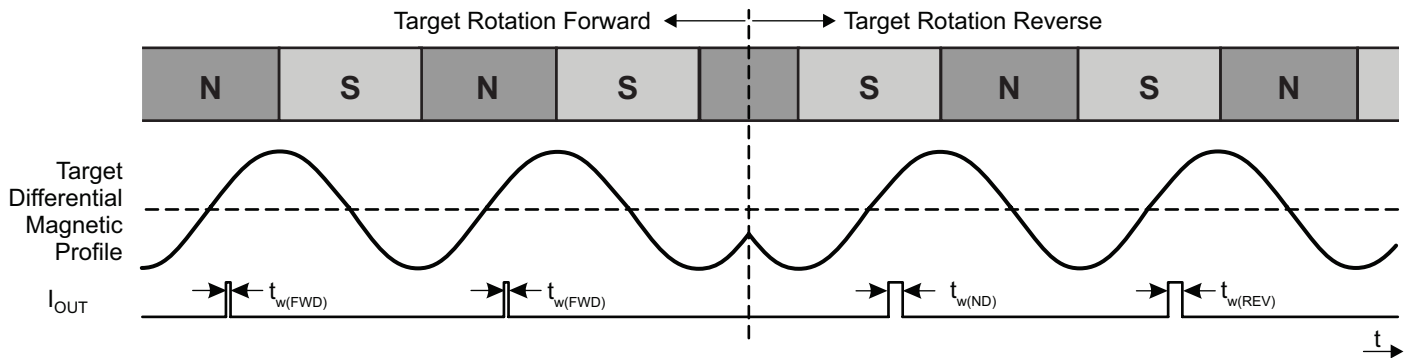


Figure 9: Example Running Mode Direction Change (-FSxxH variant)

Startup Detection/Calibration

When power is applied to the A1699, the sensor IC internally detects the profile of the target. The gain and offset of the detected signals are adjusted during the calibration period, normalizing the internal signal amplitude for the air gap range of the device.

The Automatic Gain Control (AGC) feature ensures that operational characteristics are isolated from the effects of installation air gap variation.

Automatic Offset Adjustment (AOA) is circuitry that compensates for the effects of chip, magnet, and installation offsets. This circuitry works with the AGC during calibration to adjust

VPROC in the internal A-to-D range to allow for acquisition of signal peaks. AOA and AGC function separately on the two differential signal channels.

Direction information is available after calibration is complete.

For the -xxxBx variant, the output becomes active at the end of calibration. Figure 10 shows where the first output edges may occur for various starting target phases.

For the -xxxPx variant, output pulses of $t_{W(ND)}$ are supplied during calibration. Figure 11 shows where the first output edges may occur for various starting target phases.

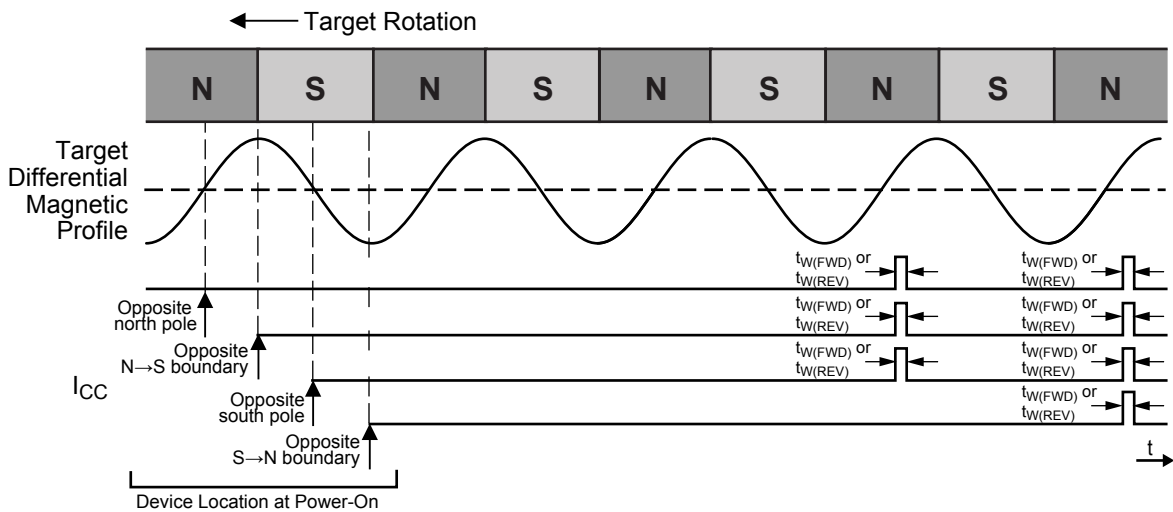


Figure 10: Startup Position Effect on First Device Output Switching (-xxxBx variant)

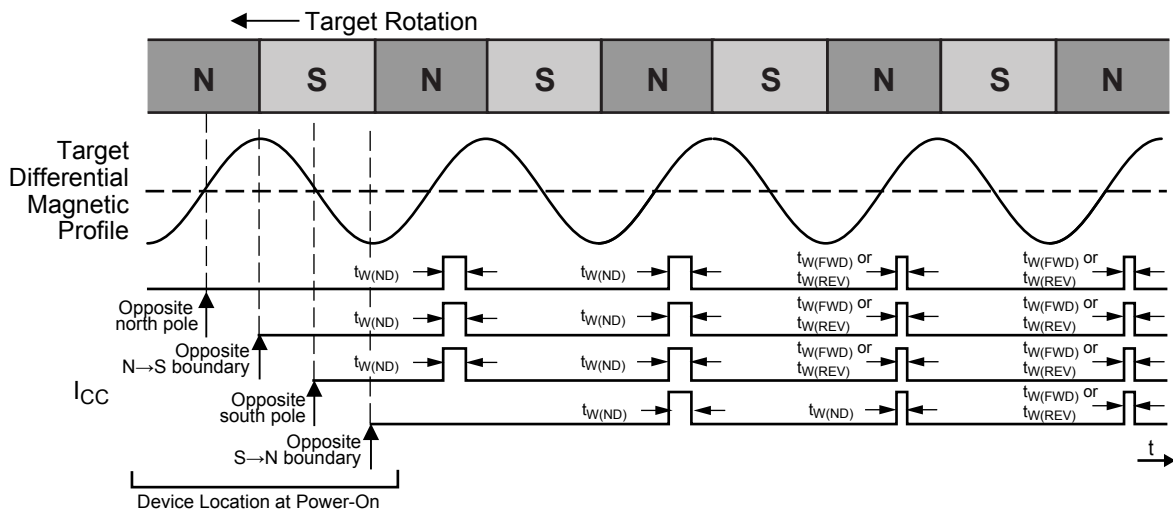


Figure 11: Startup Position Effect on First Device Output Switching (-xxxPx variant)

Vibration Detection

Algorithms embedded in the IC's digital controller detect the presence of target vibration through analysis of the two magnetic input channels.

For the -xxxxL variant, the first direction change is immediately transmitted to the output. During any subsequent vibration, the output is blanked and no output pulses will occur for vibrations less than the specified vibration immunity. Output pulses contain-

ing the proper direction information will resume when direction information is validated on constant target rotation.

For the -xxxxH variant, in the presence of vibration, output pulses of $t_w(ND)$ may occur or no pulses may occur, depending on the amplitude and phase of the vibration. Output pulses have a width of $t_w(ND)$ until direction information is validated on constant target rotation.

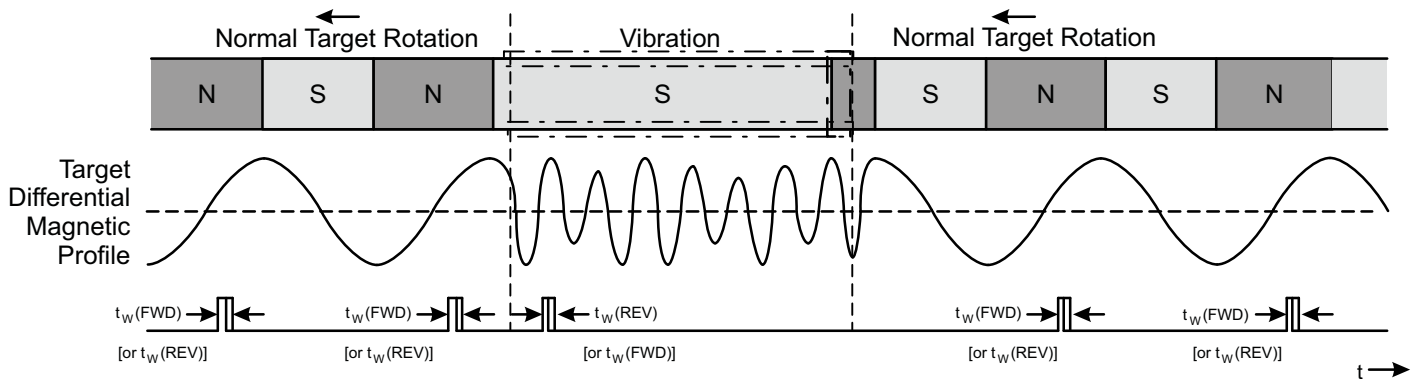


Figure 12: Output Functionality in the Presence of Running Mode Target Vibration (-xxxxL variant)

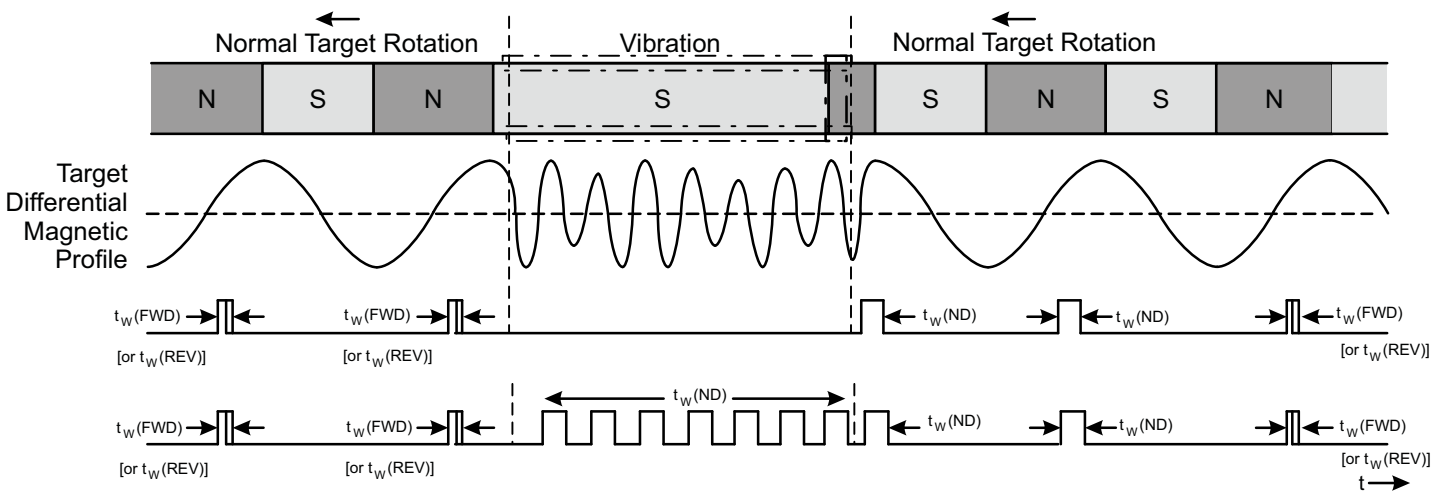


Figure 13: Output Functionality in the Presence of Running Mode Target Vibration (-xxxxH variant)

POWER DERATING

The device must be operated below the maximum junction temperature of the device, $T_{J(max)}$. Under certain combinations of peak conditions, reliable operation may require derating supplied power or improving the heat dissipation properties of the application. This section presents a procedure for correlating factors affecting operating T_J . (Thermal data is also available on the Allegro MicroSystems website.)

The Package Thermal Resistance, $R_{\theta JA}$, is a figure of merit summarizing the ability of the application and the device to dissipate heat from the junction (die), through all paths to the ambient air. Its primary component is the Effective Thermal Conductivity, UB , of the printed circuit board, including adjacent devices and traces. Radiation from the die through the device case, $R_{\theta JC}$, is relatively small component of $R_{\theta JA}$. Ambient air temperature, T_A , and air motion are significant external factors, damped by overmolding.

The effect of varying power levels (Power Dissipation, P_D), can be estimated. The following formulas represent the fundamental relationships used to estimate T_J , at P_D .

$$P_D = V_{IN} \times I_{IN} \quad (1)$$

$$\Delta T = P_D \times R_{\theta JA} \quad (2)$$

$$T_J = T_A + \Delta T \quad (3)$$

For example, given common conditions such as: $T_A = 25^\circ C$, $V_{CC} = 12 V$, $R_{\theta JA} = 213^\circ C/W$, and $I_{CC} = 6.5 mA$, then:

$$P_D = V_{CC} \times I_{CC} = 12 V \times 6.5 mA = 78 mW$$

$$\Delta T = P_D \times R_{\theta JA} = 78 mW \times 213^\circ C/W = 16.6^\circ C$$

$$T_J = T_A + \Delta T = 25^\circ C + 16.6^\circ C = 41.6^\circ C$$

A worst-case estimate, $P_{D(max)}$, represents the maximum allowable power level ($V_{CC(max)}$, $I_{CC(max)}$), without exceeding $T_{J(max)}$, at a selected $R_{\theta JA}$ and T_A .

Example: Reliability for V_{CC} at $T_A = 150^\circ C$.

Observe the worst-case ratings for the device, specifically:

$R_{\theta JA} = 213^\circ C/W$, $T_{J(max)} = 165^\circ C$, $V_{CC(max)} = 24 V$, and $I_{CC(mean)} = 14.8 mA$. (Note: For variant -xxWPx, at maximum target frequency, $I_{CC(LOW)} = 8 mA$, $I_{CC(HIGH)} = 16 mA$, and maximum pulse widths, the result is a duty cycle of 84% and thus a worst-case mean I_{CC} of 14.8 mA.)

Calculate the maximum allowable power level, $P_{D(max)}$. First, invert equation 3:

$$\Delta T_{max} = T_{J(max)} - T_A = 165^\circ C - 150^\circ C = 15^\circ C$$

This provides the allowable increase to T_J resulting from internal power dissipation. Then, invert equation 2:

$$P_{D(max)} = \Delta T_{max} \div R_{\theta JA} = 15^\circ C \div 213^\circ C/W \text{ (estimated)} = 70.4 mW$$

Finally, invert equation 1 with respect to voltage:

$$V_{CC(est)} = P_{D(max)} \div I_{CC(max)} = 70.4 mW \div 14.8 mA = 4.7 V$$

The result indicates at T_A , the application and device can dissipate adequate amounts of heat at voltages $\leq V_{CC(est)}$.

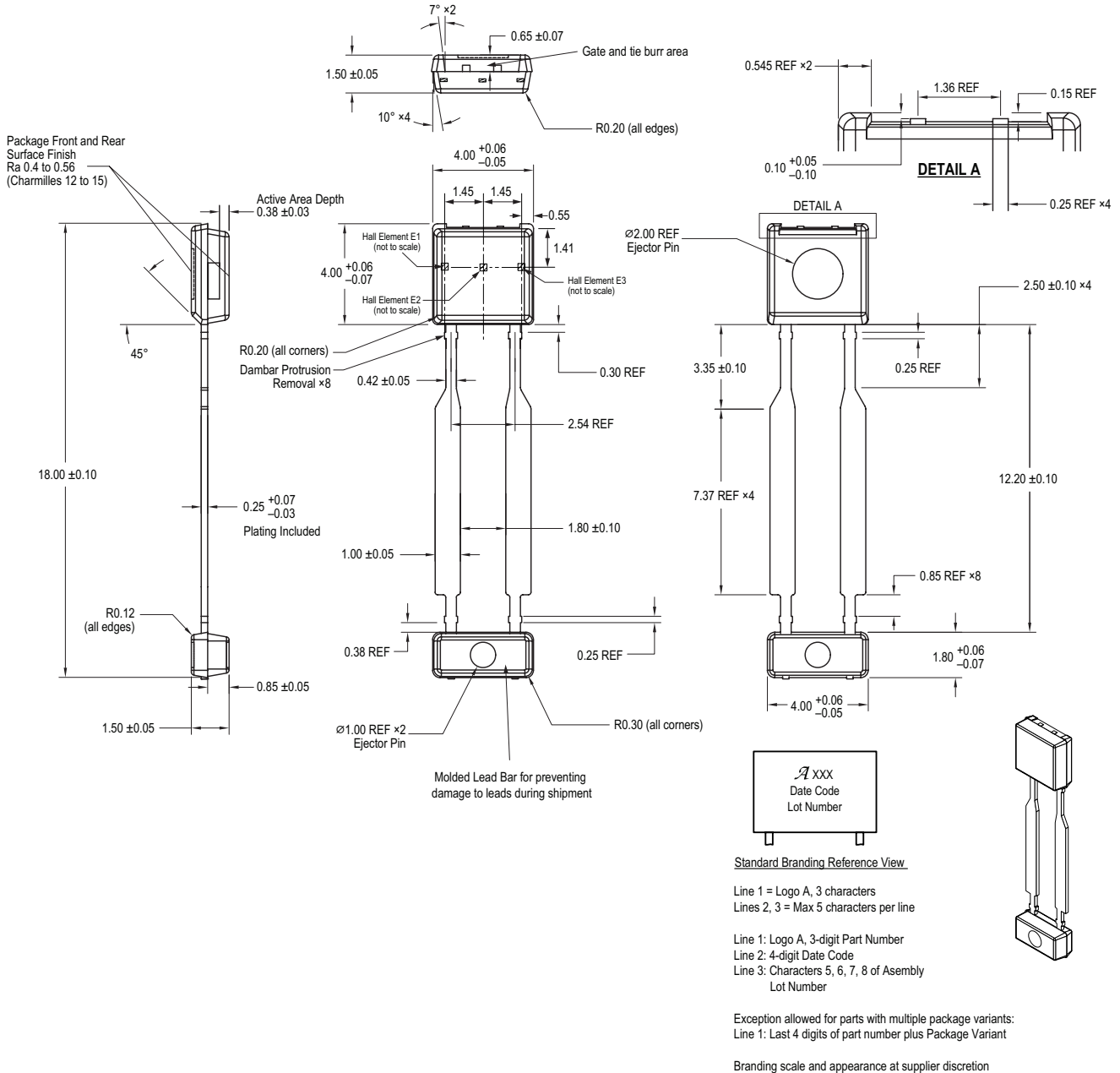
Compare $V_{CC(est)}$ to $V_{CC(max)}$. If $V_{CC(est)} \leq V_{CC(max)}$, then reliable operation between $V_{CC(est)}$ and $V_{CC(max)}$ requires enhanced $R_{\theta JA}$. If $V_{CC(est)} \geq V_{CC(max)}$, then operation between $V_{CC(est)}$ and $V_{CC(max)}$ is reliable under these conditions.

PACKAGE OUTLINE DRAWING

For Reference Only – Not for Tooling Use

(Reference DWG-0000408, Rev. 4)
Dimensions in millimeters – NOT TO SCALE

Exact case and lead configuration at supplier discretion within limits shown



Revision History

Number	Date	Description
–	March 1, 2014	Initial release.
1	October 7, 2014	Updated Package Outline Drawing and reformatted document.
2	December 12, 2014	Revised C_{SUPPLY} , t_r , and t_f .
3	March 24, 2015	Updated branding on Package Outline Drawing.
4	September 23, 2015	Updated Hall element number and positions in top outline of Package Outline Drawing; updated Figures 6 and 7 and associated text on page 12; updated Pulse Width Characteristic Performance plots on page 10; removed bulk offering on page 2-3; additional editorial changes.
5	March 1, 2016	Updated Package Outline Drawing molded lead bar footnote and Internal Discrete Capacitor Ratings table.
6	April 7, 2016	Corrected Figure 6 and 7 captions.
7	September 23, 2016	Updated Package Outline Drawing.
8	April 3, 2019	Minor editorial updates
9	April 4, 2022	Updated package drawing (page 17)

Copyright 2022, Allegro MicroSystems.

Allegro MicroSystems reserves the right to make, from time to time, such departures from the detail specifications as may be required to permit improvements in the performance, reliability, or manufacturability of its products. Before placing an order, the user is cautioned to verify that the information being relied upon is current.

Allegro's products are not to be used in any devices or systems, including but not limited to life support devices or systems, in which a failure of Allegro's product can reasonably be expected to cause bodily harm.

The information included herein is believed to be accurate and reliable. However, Allegro MicroSystems assumes no responsibility for its use; nor for any infringement of patents or other rights of third parties which may result from its use.

Copies of this document are considered uncontrolled documents.

For the latest version of this document, visit our website:

www.allegromicro.com